galaxies in our sample are larger than 1.2 arc min in diameter, there is no obvious trend for worse classification for smaller diameters, although such a trend is expected for much smaller galaxies. There is also no dramatic trend with ellipticity. Of the 831 galaxies classified by the ANN by the above procedure, 9% deviate from the "true" mean answer by at least three types. Most of them are very late types and irregulars ($T > 7$).

Our comparison indicates that although the T-system is convenient, the scatter between observers is not negligible. Caution is called for in assuming a universal frequency type distribution in comparison with models and with high-redshift galaxies. The observed frequency distribution depends on the plate material and on the human expert. Future work will focus on supervised ANNs, to preserve human experience in multidimensional classification (*3*, *5*), and on unsupervised algorithms (for example, by generalizing principal component analysis to nonlinear mapping), to define a "new physical Hubble sequence" without any prior human classification.

REFERENCES AND NOTES

1. E. Hubble, *The Realm of Nebulae* (Yale Univ. Press, New Haven, CT, 1936).
2. A. R. Sandage, *The Hubble Atlas of Galaxies* (Carnegie Institute of Washington, Washington, DC, 1961).
3. G. de Vaucouleurs, *Hand. Phys.* **53**, 275 (1959).
4. W. W. Morgan, *Publ. Astron. Soc. Pac.* **70**, 364 (1958).
5. S. van den Bergh, *Astrophys. J.* **206**, 883 (1976).
6. R. Buta, S. Mitra, G. de Vaucouleurs, H. G. Corwin Jr., *Astron. J.* **107**, 118 (1994).
7. A. Dressler, *Astrophys. J.* **236**, 351 (1980).
8. R. B. Tully and J. R. Fisher, *Astron. Astrophys.* **54**, 661 (1977).
9. D. Lynden-Bell *et al.*, *Astrophys. J.* **326**, 19 (1988).
10. G. de Vaucouleurs *et al.*, *Third Reference Catalogue of Bright Galaxies* (Springer-Verlag, New York, 1991).
11. A. Lauberts and E. A. Valentijn, *The Surface Photometry Catalogue of the ESO-Uppsala Galaxies* (European Southern Observatory, Munich, 1989).
12. M. Thonnat, in *The World of Galaxies*, H. G. Corwin and L. Bottinelli, Eds. (Springer-Verlag, New York, 1988), p. 53.
13. G. Spiekermann, *Astron. J.* **103**, 2102 (1992).
14. M. C. Storrie-Lombardi, O. Lahav, L. Sodré Jr., L. J. Storrie-Lombardi, *Mon. Not. R. Astron. Soc.* **259**, 8 (1992).
15. M. Doi, M. Fukugita, S. Okamura, *ibid.* **264**, 832 (1993).
16. R. Abraham, F. Valdes, H. K. C. Yee, S. van den Bergh, *Astrophys. J.* **432**, 75 (1994).
17. S. Raychaudhury *et al.*, in preparation.
18. In the T-type system of galaxy classification (*10*), the types $T = -6$ to 9 correspond to galaxy types *cE*, *E0*, *E+*, *S0⁻*, *S0⁰*, *S0⁺*, *S0/a*, *Sa*, *Sab*, *Sb*, *Sbc*, *Sc*, *Scd*, *Sd*, *Sdm*, and *Sm*, respectively; types $T = 10$, 11, 90, and 99 correspond to *Im*, *cI*, *I0*, and *Pec*, respectively.
19. A. Naim *et al.*, in preparation.
20. J. Hertz, A. Krogh, R. G. Palmer, *Introduction to the Theory of Neural Computation* (Addison-Wesley, Redwood, CA, 1991).
21. S. C. Odewahn, E. B. Stockwell, R. L. Pennington, R. M. Humphreys, W. A. Zumach, *Astron. J.* **103**, 318 (1992).
22. M. Serra-Ricart, X. Calbet, L. Garrido, V. Gaitan, *ibid.* **106**, 1685 (1993).
23. D. E. Rumelhart, G. E. Hinton, R. J. Williams, *Nature* **323**, 533 (1986).
24. O. Lahav, A. Naim, L. Sodré Jr., M. C. Storrie-Lombardi, in preparation.
25. A. Naim, O. Lahav, L. Sodré Jr., M. C. Storrie-Lombardi, in preparation.

26. We thank the Schmidt Telescope unit of the Royal Observatory of Edinburgh for the plate material, the APM group at the Royal Greenwich Observatory, Cambridge, for scanning support, M. Irwin and D. Lynden-Bell for helpful discussions. We are also grateful to the anonymous referee for helpful comments.

16 August 1994; accepted 1 December 1994

Temperature Dependence of the Superconducting Gap Anisotropy in $Bi_2Sr_2CaCu_2O_{8+x}$

Jian Ma, C. Quitmann, R. J. Kelley, H. Berger, G. Margaritondo, M. Onellion*

Detailed data on the momentum-resolved temperature dependence of the superconducting gap of $Bi_2Sr_2CaCu_2O_{8+x}$ are presented, complemented by similar data on the intensity of the photoemission superconducting condensate spectral area. The gap anisotropy between the Γ-M̄ and Γ-X directions increases markedly with increasing temperature, contrary to what happens for conventional anisotropic-gap superconductors, such as lead. Specifically, the size of the superconducting gap along the Γ-X direction decreases to values indistinguishable from zero at temperatures for which the gap retains virtually full value along the Γ-M̄ direction. These data rule out the simplest type of *d*-wave order parameter.

An "order parameter" describes the type of phase transition that occurs in a material system. The order parameter of high-temperature superconductors is of extreme current interest and has been investigated by several techniques, including angle-resolved photoemission (*1*–*4*). Angle-resolved photoemission has the advantage of directly investigating the momentum dependence of the gap. Already, results establishing a marked anisotropy in the gap at low temperatures have ruled out an isotropic *s*-wave symmetry order parameter (*2*–*5*).

Our main result is that, contrary to conventional anisotropic-gap superconductors such as lead (*6*), the gap anisotropy of oxygen-overdoped $Bi_2Sr_2CaCu_2O_{8+x}$ increases with increasing temperature as one approaches the superconducting transition temperature T_c. We estimated the size of the gap in two ways: using the BCS (Bardeen-Cooper-Schrieffer)-like lineshape (*1*, *7*) computer code of Olson *et al.* (*1*) and also using the shift of the 50% point of the photoemission leading edge (*2*). The gap values obtained by the two methods agreed to better than 1.5 meV. Our results place stringent constraints on any theory of high-temperature superconductivity.

J. Ma, C. Quitmann, R. J. Kelley, M. Onellion, Department of Physics and Applied Superconductivity Center, University of Wisconsin–Madison, 1150 University Avenue, Madison, WI 53706, USA.
H. Berger and G. Margaritondo, Institut de Physique Appliquée, Ecole Polytechnique Fédérale, CH-1015 Lausanne, Switzerland.

*To whom correspondence should be addressed.

As a test of our experimental standards, we measured the angle-resolved photoemission spectrum of a gold film deposited in situ (Fig. 1A); the temperature of the film was 36 K. The 10 to 90% energy width of the Fermi-Dirac distribution function Fermi edge was 15 ± 2 meV. Magnetic susceptibility measurements were also taken for an oxygen-overdoped $Bi_2Sr_2CaCu_2O_{8+x}$ single crystal sample (Fig. 1B) as part of a test of sample quality. The 10 to 90% transition temperature width was 1.3 K. Our photoemission measurements were performed in an ultrahigh-vacuum chamber with a base pressure of 6×10^{-11} torr. The light source was the 4-m normal incidence monochromator at the Wisconsin Synchrotron Radiation Center. The electron energy analyzer we used was a 50-mm Vacuum Science Workshop hemispherical analyzer, mounted on a two-axis goniometer, with an acceptance full angle of 2°. The total energy resolution employed was 25 meV, slightly worse than the best obtainable. Samples were transferred from a load lock chamber and were cleaved in situ at 35 K. The sample holder rotated the sample about the surface normal, at low temperature, for precision alignment with respect to the photon electric field. The sample crystal structure and orientation were determined by in situ low-energy electron diffraction (LEED). The sample temperature stability was ±1 K.

For measurements of the temperature dependence of the gap, we chose two locations in the Brillouin zone where the superconducting gap is large. These points are (i)

along the Γ-M̄ [(100)] direction (the Cu–O–Cu bond axis in real space) near M̄, at wave vector $k_x = 0.92$ Å^{-1}, and (ii) along the Γ-X [(110)] direction (the Bi–O–Bi direction, without superlattice structure, in real space) at $k_x = k_y = 0.33$ Å^{-1}. Figure 2 illustrates the angle-resolved photoemission data (raw data, without smoothing) taken along the Γ-M̄ direction for temperatures from 36 to 95 K. The count rate in the photoemission superconducting condensate spectral area at 36 K was about 1 kHz. The main temperature-dependent features of these spectra include a shift of the leading edge that reveals the opening of the superconducting gap, a photoemission superconducting condensate spectral area with an energy full width at half maximum of 25 meV immediately below the leading edge, and a dip at a binding energy of about 80 meV (*2*, *3*) for temperatures up to $0.84T_c$. Along the Γ-M̄ direction, the photoemission superconducting condensate spectral area disappears above the transition temperature $T_c = 83$ K but has been reproducibly observed at temperatures within 2 K of T_c. Using the Olson-Lynch-Liu code (*1*), we find that the gap opens quite rapidly below the bulk transition temperature T_c, reaching its full value at $0.85T_c$.

The results of Fig. 2 are in striking contrast to the corresponding results obtained along the Γ-X symmetry direction (Fig. 3). Along this direction, the photoemission superconducting condensate spectral area is weaker, and the shift of the leading edge of the spectrum at 40 K is significantly less than that along the Γ-M̄ direction. At temperatures well below T_c, there is a nonzero superconducting gap (Fig. 3B). This is a significant point: It rules out the simplest type of *d* symmetry order parameter, specifically pure $d_{x^2-y^2}$, well below T_c (*8*, *9*). On the other hand, the gap becomes indistinguishable from zero along the Γ-X direction

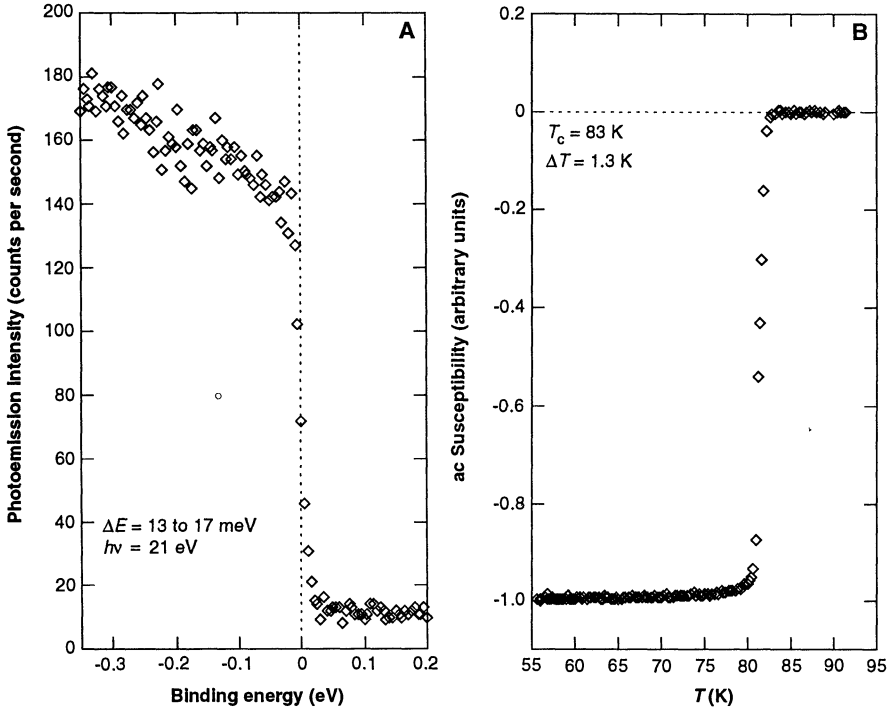

Fig. 1. (**A**) Gold Fermi edge photoemission spectrum measured at 36 K. The 10 to 90% width is 15 ± 2 meV. (**B**) Magnetic susceptibility data for our $Bi_2Sr_2CaCu_2O_{8+x}$ single crystal.

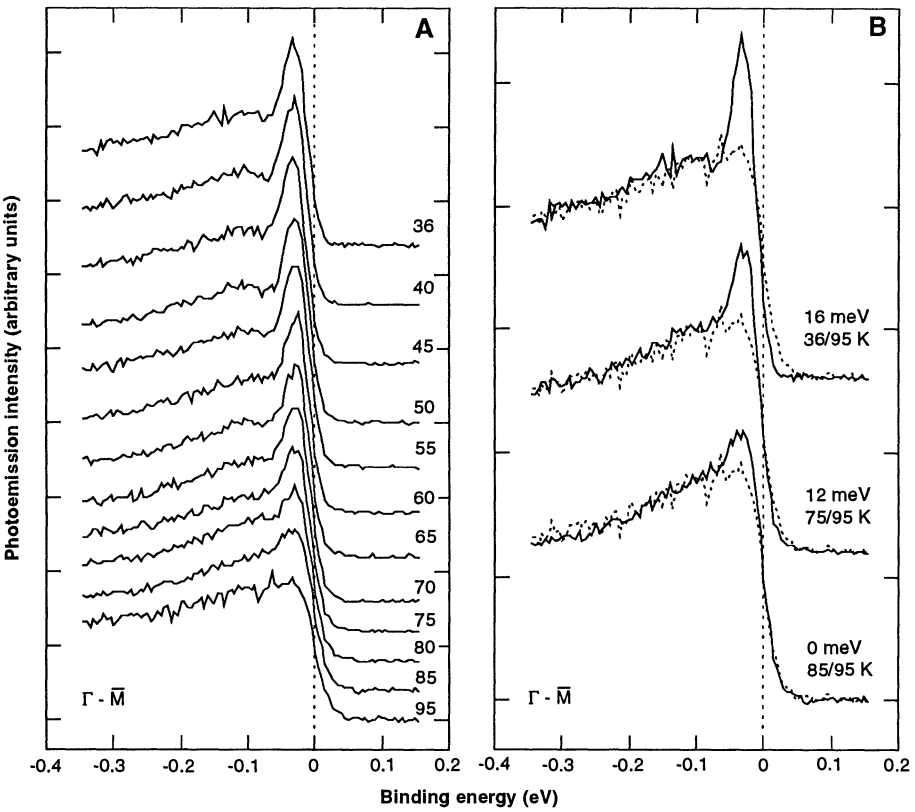

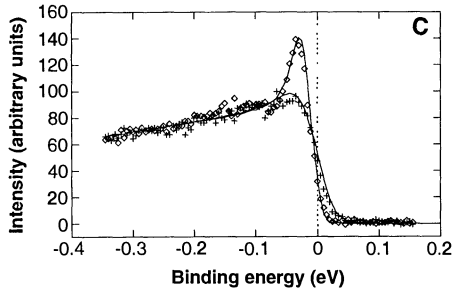

Fig. 2. (**A**) Angle-resolved photoemission spectra versus temperature for the $(k_x, k_y) = (0.92$ Å$^{-1}, 0.0$ Å$^{-1})$ location along the Γ-M̄ direction. The photon energy was 21 eV. The data were taken from 36 K ($0.40T_c$) to 95 K ($1.15T_c$). (**B**) Direct comparison of the spectra at 36, 75, and 85 K (solid) to that at 95 K (dotted). The superconducting gap Δ obtained for each spectrum is noted above the temperatures. (**C**) Spectra taken at 36 and 95 K, compared to the best fit from the BCS fitting algorithm.

at a temperature (70 K) for which the gap is still at 90 to 100% of full value along the Γ-M̄ direction (Fig. 4).

The gap anisotropy between the Γ-M̄ and Γ-X directions increases with increasing temperature (Fig. 4A). For the Γ-M̄ direction, the gap is still visible for temperatures as high as $0.94T_c$ to $0.98T_c$ and retains its full value up to $(0.82 \pm 0.03)T_c$. By contrast, in the Γ-X direction, the gap begins to decrease at $(0.57 \pm 0.03)T_c$ and is indistinguishable from zero at $0.81T_c$. Consequently, the gap anisotropy, already present at low temperatures, increases as the temperature approaches T_c. With the most conservative error bars, the gap anisotropy for the two directions increases from 1.8 at $0.40T_c$ to 14 at $0.85T_c$, an increase of at least a factor of 8.

The size of the gap in the Γ-X direction varied with oxygen concentration, ranging from between 0 and 2 meV for underdoped and optimally doped samples to between 8 and 12 meV for overdoped samples (*10*). Earlier reports have noted that the gap size along the Γ-X direction appears to vary with oxygen content (*1*, *5*). Because the gap along Γ-X is so small, even at lower temperatures, we have not studied the temperature dependence of the gap along Γ-X for underdoped samples. We have studied the temperature dependence of the gap along Γ-M̄ for underdoped samples and find it similar to the data of Fig. 4A.

We made several checks to ensure that the differences illustrated in Fig. 4A are due to the different symmetry directions. We observed a temperature dependence of the momentum-resolved photoemission superconducting condensate spectral area n_s. The value of n_s is proportional to the number of electrons that are removed by the superconducting transition from an energy domain roughly equal to the gap (Cooper pairs form at energies immediately below the gap). We obtained n_s by subtracting the normal state (quasi-particle) spectral area from the superconducting state spectral area between 10 and 55 meV of binding energy. The change in n_s with temperature (Fig. 4B) was a robust quantity, not sensitive to exactly what binding energy range was used to define the photoemission superconducting condensate spectral area. Although there is no detailed theoretical calculation of $n_s(T)$, several noteworthy points emerge from the data. At $0.40T_c$, n_s is nonzero in both the Γ-M̄ and Γ-X directions, as expected for a nonzero gap in both directions (*2*, *4*). As the temperature increases from the lowest temperature, n_s goes down more rapidly in the Γ-X direction than in the Γ-M̄ direction, particularly between $0.50T_c$ and $0.80T_c$. When the gap in the Γ-X direction becomes very small (Fig. 4A), n_s in the Γ-X direction drops to virtually zero (Fig. 4B). Furthermore, n_s in the Γ-X direction is indistinguishable from zero for temperatures at which n_s in the Γ-M̄ direction is still appre-

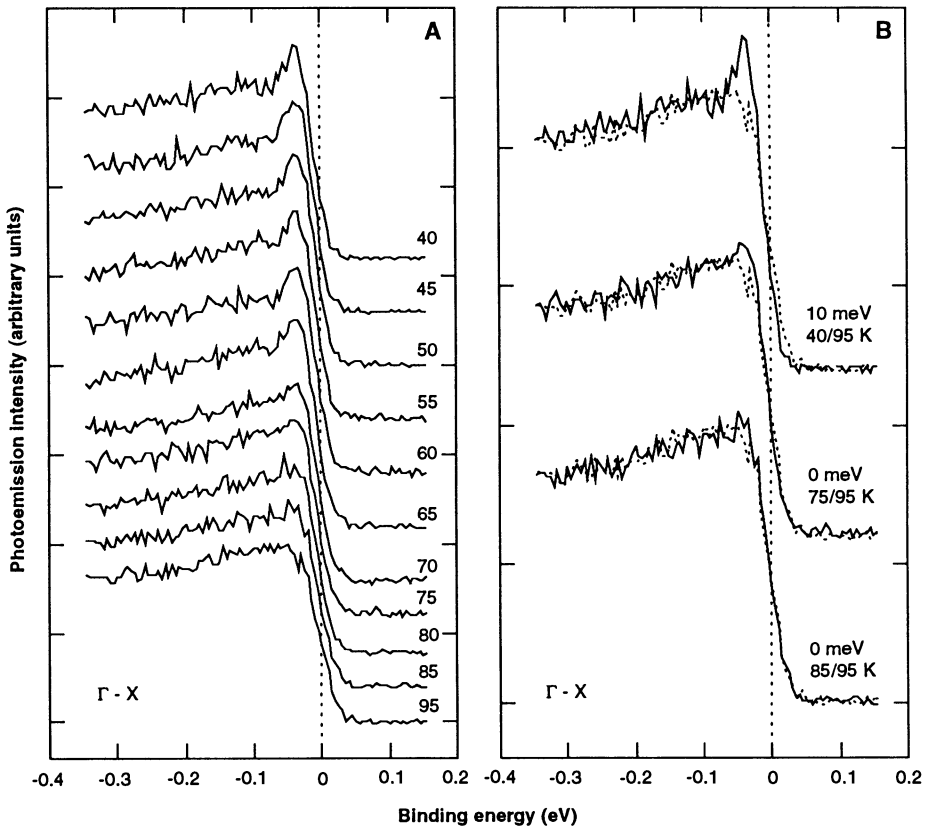

Fig. 3. (**A**) Angle-resolved photoemission spectra versus temperature for the (k_x, k_y) = (0.33 Å^{-1}, 0.33 Å^{-1}) location along the Γ-X direction. A photon energy of 21 eV was used. The data were taken from 40 K ($0.46T_c$) to 95 K ($1.15T_c$). (**B**) Direct comparison of the spectra at 40, 75, and 85 K (solid) to that at 95 K (dotted). The superconducting gap Δ obtained for each spectrum is noted above the temperatures. At 75 K, the gap is zero, whereas for the Γ-M̄ direction (Fig. 2B), it is nonzero. (**C**) Spectra taken at 40 and 95 K, compared to the best fit from the BCS fitting algorithm.

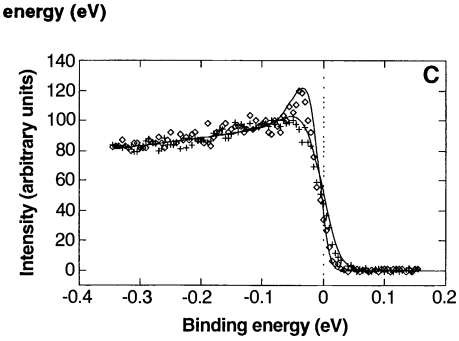

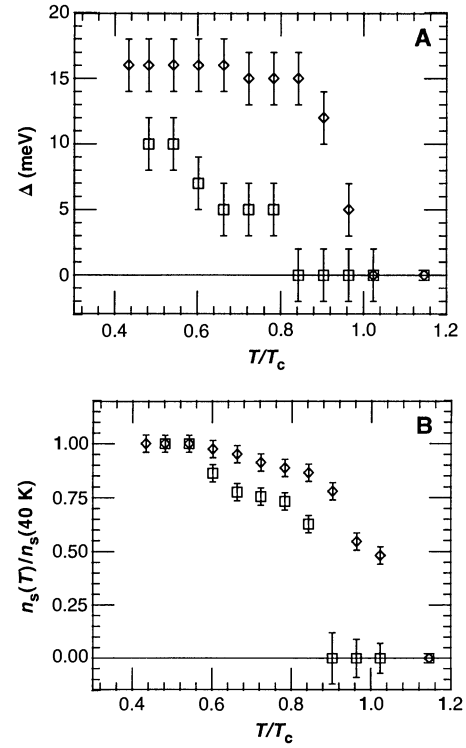

Fig. 4. (**A**) The size of the superconducting gap Δ for the Γ-M̄ direction (diamonds) and the Γ-X direction (squares) as a function of temperature. The gap remains at full value up to $0.85T_c$ along the Γ-M̄ direction but is reduced along the Γ-X direction starting at $0.57T_c$, reaching zero at $0.82T_c$. (**B**) The intensity n_s, defined as the difference in photoemission spectral area between the superconducting state and normal quasi-particle state, versus temperature for the Γ-M̄ direction (diamonds) and the Γ-X direction (squares). The plot is normalized to the value of n_s at 40 K. Note that n_s decreases faster in the Γ-X direction, dropping markedly above $0.80T_c$, compared with the Γ-M̄ direction.

ciable. The behavior of n_s mirrors the temperature dependence of the gap anisotropy. The nonzero values of n_s near T_c are consistent with those of Dessau *et al.* (*5*) and, we speculate, may be due to superconducting fluctuations.

As an additional check, we fabricated samples with different oxygen and cation stoichiometries. Different samples exhibited the same size gap at low temperatures, one in the Γ-M̄ and another in the Γ-X direction. We found a growing gap anisotropy with increasing temperature, the same behavior as in Fig. 4A.

We also checked the effect of the normal state (quasi-particle) binding energy. We compared samples where the quasi-particle binding energy along the Γ-M̄ direction of one sample and that along the Γ-X direction of a different sample were the same. The difference illustrated in Fig. 4 persisted. We conclude that the difference is related to the two symmetry directions, rather than the absolute size of the superconducting gap or the quasi-particle binding energy from which the photoemission superconducting condensate arises.

Because quantitative calculations comparing to our experimental data of Figs. 2 through 4 are not currently available, we neither endorse nor rule out specific models (*8*, *9*, *11*–*15*). Instead, we note how various models are constrained by our results. Any model must explain how the gap anisotropy arises. More stringent is that any model must explain how the anisotropy changes from 1.8:1 at $0.40T_c$ to at least 14:1 at $0.85T_c$, a change of a factor of 8 or 9. The increasing gap anisotropy as the temperature approaches T_c is a peculiar feature of high-temperature superconductors. A conventional BCS superconductor such as lead can have a gap anisotropy at low temperatures (*6*); however, this anisotropy disappears as T_c is approached from below (*6*).

Our data can be interpreted in terms of a two-component order parameter (*6*), of which there are several models (*13*, *16*). One possibility is a model that exhibits only a $d_{x^2-y^2}$ symmetry component near T_c and both components at lower temperatures. It is noteworthy that the best fit to our data at 70 K and above along the Γ-X direction yields a zero gap (*8*, *9*).

However, such two-component models (*13*, *16*) do not yet provide a quantitative analysis of the temperature dependence of the two components. Earlier theoretical work on the superconducting order parameter symmetry (*14*) indicates that two transition temperatures should be observed for a two-component order parameter. We note a recent, unpublished mean field analysis of a two-component order parameter (*15*); the investigators assumed an order parameter that is a mixture of *s*- and *d*-wave components. Minimization of the corresponding Ginzburg-Landau free energy gives a temperature-dependent gap anisotropy.

REFERENCES AND NOTES

1. C. G. Olson *et al.*, *Science* **245**, 731 (1989).
2. Z.-X. Shen *et al.*, *Phys. Rev. Lett.* **70**, 1553 (1993).
3. Y. Hwu *et al.*, *ibid.* **67**, 2573 (1991).
4. R. J. Kelley, J. Ma, G. Margaritondo, M. Onellion, *ibid.* **71**, 4051 (1993).
5. D. S. Dessau *et al.*, *ibid.* **66**, 2160 (1991).
6. B. L. Blackford, *Physica* **55**, 475 (1971), particularly figure 4; *Phys. Rev. B* **5**, 1171 (1972); _____ and R. H. March, *Phys. Rev.* **186**, 397 (1969).
7. Y. Chang *et al.*, *Phys. Rev. B* **39**, 4740 (1989).
8. A. V. Chubukov and S. Sachdev, *Phys. Rev. Lett.* **71**, 169 (1993).
9. P. Monthoux and D. Pines, *Phys. Rev. B* **49**, 4261 (1994), and references therein.
10. R. J. Kelley *et al.*, in preparation.
11. G. D. Mahan, *Phys. Rev. Lett.* **71**, 4277 (1993), and references therein.
12. A. A. Abrikosov, *Physica C* **214**, 107 (1993).
13. S. Chakravarty, A. Sudbø, P. W. Anderson, S. Strong, *Science* **261**, 337 (1993).
14. J. F. Annett, *Adv. Phys.* **39**, 83 (1990).
15. J. Betouras and R. Joynt, unpublished material.
16. The idea of a two-component order parameter has been applied for heavy fermion systems. See, for example, R. Joynt, *Phys. Rev. Lett.* **71**, 3015 (1993), and references therein.

17. We thank D. Lynch, C. Olson, and R. Liu, who made their computer code on the superconducting gap available for us. C. Olson kindly showed us his heater design. We benefited from H. Ding's and R. Liu's advice about improving electron energy analyzer resolution. M. Winokur kindly showed us the use of GNUPLOT graphics. A. Umezawa supervised our ac susceptibility measurements. We benefited from conversations with R. Schrieffer, J. Annett, A. Chubukov, R. Klemm, R. Dynes, N. Goldenfeld, A. Gurevich, K. Johnson, R. Joynt, D. Pavuna, and D. Tanner. The staff of the Wisconsin Synchrotron Radiation Center (SRC), particularly R. Pedley, was most helpful. Financial support was provided by the U.S. National Science Foundation, both directly (DMR-9214707) and through support of the SRC (DMR-9212658) by Ecole Polytechnique Fédérale Lausanne and the Fonds National Suisse de la Recherche Scientifique, and by Deutsche Forschungsgemeinschaft.

8 September 1994; accepted 1 December 1994

A Neutral Templating Route to Mesoporous Molecular Sieves

Peter T. Tanev and Thomas J. Pinnavaia*

A neutral templating route for preparing mesoporous molecular sieves is demonstrated based on hydrogen-bonding interactions and self-assembly between neutral primary amine micelles (S°) and neutral inorganic precursors (I°). The S° I° templating pathway produces ordered mesoporous materials with thicker framework walls, smaller x-ray scattering domain sizes, and substantially improved textural mesoporosities in comparison with M41S materials templated by quaternary ammonium cations of equivalent chain length. This synthetic strategy also allows for the facile, environmentally benign recovery of the cost-intensive template by simple solvent extraction methods. The S° I° templating route provides for the synthesis of other oxide mesostructures (such as aluminas) that may be less readily accessible by electrostatic templating pathways.

Mobil Oil Corporation researchers discovered the M41S family of mesoporous molecular sieves from a self-assembly process involving electrostatic interactions between positively charged quaternary ammonium micelles and inorganic anions as framework precursors (*1*). Recently, Schüth, Stucky, and their co-workers (*2*) extended the electrostatic assembly approach by proposing four complementary synthesis pathways.

Pathway 1 involved the direct cocondensation of a cationic surfactant (S^+) with anionic inorganic species (I^-) to produce assembled ion pairs (S^+ I^-). The original synthesis of MCM-41 silicates is a prime example of this pathway (*1*). In the charge-reversed situation (pathway 2), an anionic template (S^-) was used to direct the self-assembly of cationic inorganic species (I^+) through S^- I^+ ion pairs. Pathways 3 and 4 involved counterion (X^- or M^+)–mediated assemblies of surfactants and inorganic species of similar charge. These counterion-mediated pathways produced assembled solution species of the type S^+ X^- I^+ (where X^- = Cl^- or Br^-) or S^- M^+ I^- (where M^+ = Na^+ or K^+), respectively. The viability of pathway 3 was demonstrated by the synthesis of a hexagonal MCM-41 silica with quaternary ammonium cations under strongly acidic conditions (5 to 10 M HCl or HBr) to generate and assemble positively charged framework precursors (*2*). Also, we have reported (*3*) the preparation of a mesoporous silica molecular sieve and a Ti-substituted analog by the acid-catalyzed hydrolysis of inorganic alkoxide precursors in the presence of primary ammonium ions.

Department of Chemistry and Center for Fundamental Materials Research, Michigan State University, East Lansing, MI 48824, USA.

*To whom correspondence should be addressed.